

Magnetic mesoporous carbon composites incorporating hydrophilic metallic nanoparticles for enrichment of phosphopeptides prior to their determination by MALDI-TOF mass spectrometry

Lei Zhang¹ · Yangyang Gan¹ · Haofan Sun¹ · Bohao Yu¹ · Xiaofeng Jin² · Runsheng Zhang³ · Weibing Zhang¹ · Lingyi Zhang¹

Received: 13 July 2016 / Accepted: 5 December 2016 / Published online: 10 December 2016
© Springer-Verlag Wien 2016

Abstract Magnetic mesoporous carbon composites incorporating hydrophilic metallic nanoparticles were synthesized from resorcinol, ZrO(NO₃)₂, ferric acetylacetonate, and triblock copolymer F127. The method involves a multi-component co-assembly strategy associated with direct carbonization. The resulting carbon material is shown to be useful as a metal oxide affinity chromatography (MOAC) material for enrichment of phosphopeptides owing to its large mesoporous (4.8 nm) surface area (442 m² g⁻¹), large pore volume (0.37 cm³ g⁻¹) and excellent hydrophilicity. The metallic iron and ferric oxide particles modified on the mesoporous carbon exert a magnetic force and, in combination with the metallic zirconia, is a viable MOAC material for enrichment of low-abundance phosphopeptides. Because of metal chelation between metallic nanoparticles and the phosphate groups of phosphopeptides, the zirconia/magnetic mesoporous carbon displays high

selectivity even at a phosphopeptide/nonphosphopeptide molar ratio of 1:500. As little as 1.5 fmol of phosphopeptides become detectable. The MOAC was successfully applied to the identification by MALDI-TOF MS of phosphopeptides in human serum and nonfat milk.

Keywords Magnetic mesoporous carbon · Ferric oxide · Zirconia · Nanoparticles · Hydrophilic carbon material · Metal oxide affinity chromatography · Phosphopeptide · Enrichment · Human serum · MALDI-TOF MS

Introduction

Phosphorylation is one of the protein post-translational modifications [1] that is a key regulator of cell cycling, cell growth, cell differentiation and metabolism [2]. It is also involved in several diseases including cancers [3], Alzheimer's disease [4] and diabetes [5]. The detection of low-abundance phosphopeptides is one of the most important research fields [6–8]. High abundant proteins from the complex biological samples always had severe interference to the detection of low-abundance phosphopeptides which were connected with some diseases. Therefore, it is urging for the removal of high-abundance protein or peptides and enrichment of low-abundance phosphopeptides.

Numerous strategies have been developed for the enrichment of phosphopeptides. These include immobilized metal ion affinity chromatography (IMAC) [9, 10], molecularly imprinted [11, 12], chemical modification [13], strong cation exchange (SCX) [14, 15], strong anion exchange (SAX) [16], amine-based affinity [17] and metal oxide affinity chromatography (MOAC) [18]. Because of the excellent combining capacity between metal oxides and

Electronic supplementary material The online version of this article (doi:10.1007/s00604-016-2046-6) contains supplementary material, which is available to authorized users.

✉ Weibing Zhang
weibingzhang@ecust.edu.cn

✉ Lingyi Zhang
zhanglingyi@ecust.edu.cn

¹ Shanghai Key Laboratory of Functional Materials Chemistry, School of Chemistry & Molecular Engineering, East China University of Science and Technology, Shanghai 200237, China

² China National Quality Supervision and Testing Center for Cu-Pb-Zn and Products, 1991 CuiHu Five Road, Tongling, Anhui 244000, China

³ Shanghai Key Laboratory of Crime Scene Evidence, Shanghai Research Institute of Criminal Science and Technology, Shanghai Public Security Bureau, 803 ZhongShan North One Road, Shanghai 200042, China

phosphate groups in acidic environment, MOAC is one of the most commonly used methods [19]. Lots of metal oxides, such as TiO_2 [20], ZrO_2 [21], Fe_2O_3 [22], Ta_2O_5 [23] and HfO_2 [24], were acted as MOAC material for enrichment of phosphopeptides. For example, Kailasa [25] et al. used BaTiO_3 NPs as MOAC material for the enrichment of phosphopeptides from microwave tryptic digests of α -casein and non-fat milk.

As for MOAC, many matrixes were used to load metal oxides in the phosphopeptides enrichment, such as magnetic Fe_3O_4 , graphene oxide, yolk-shell structural magnetic nanocomposites and mesoporous silica nanotubes. For example, Long [26] et al. use the magnetic Fe_3O_4 as matrix to synthesize core-shell structured magnetic lutetium phosphate ($\text{Fe}_3\text{O}_4@ \text{LuPO}_4$) affinity microspheres to selectively enrich phosphopeptides for MALDI-TOF MS analysis. Huang [27] et al. reported a graphene oxide induced growth of fusiform zirconia nanostructures for capture of phosphopeptides. Wan [28] et al. synthesized magnetic yolk-shell ($\text{Fe}_3\text{O}_4@m\text{TiO}_2@m\text{SiO}_2$ nanocomposites) for selective enrichment of endogenous phosphopeptides. Zhang [29] et al. prepared zirconia layer coated with mesoporous silica nanotubes (ZrO_2 -MSN) for the enrichment of phosphopeptides. Among these matrixes, the magnetic Fe_3O_4 had the advantage in quick magnetic separation, but the relatively low surface areas limits the loading of metal oxides. Graphene oxide, mesoporous silica nanotubes or ordered mesoporous carbon own large surface areas for metal oxides loading, however, they required laborious separation procedure (e.g. centrifugation), which is inconvenient and may lead to undesirable non-specific peptides and loss of low-abundance phosphopeptides.

In our previous work [30], hydrophilic nanostructure metallic zirconia incorporated ordered mesoporous carbon composites were synthesized via soft template of multi-component co-assembly strategy. The zirconia/OMC composites had lots of merits such as large mesoporous (5.6 nm), high surface area ($387 \text{ m}^2 \text{ g}^{-1}$), large pore volume ($0.35 \text{ cm}^3 \text{ g}^{-1}$), high loading content of metallic zirconia (3.5 wt%) and high hydrophilicity for selective enrichment low abundant phosphopeptides. Herein, based on the previous works, the metallic nanoparticles iron and ferric oxides were introduced to the surface of mesoporous carbon to form the metallic nanoparticles-incorporated magnetic mesoporous carbon composites. The ferric oxides were regarded as both the magnetic source and the metal oxide affinity chromatography material for enrichment low-abundance phosphopeptides. The obtained nanocomposites possess a suitable pore structure, high surface area, moderate pore volume and uniform and highly dispersed metallic oxides. Because of the highly dispersed metallic mesoporous carbon and excellent hydrophilicity, the material was suitable for enrichment phosphopeptides.

Materials and methods

Apparatus

The metallic zirconia incorporated magnetic mesoporous carbon composites structure and surface morphology of microspheres were studied with ultrahigh resolution field emission scanning electron microscopy (<https://www.fei.com>, UHRFESEM, NOVA Nano SEM450, FEI, USA) and ultrahigh resolution transmission electron microscope (<http://www.jeol.co.jp>, HR-TEM, JEM-2100, JEOL, Japan). The crystalline structure of material was characterized by D/MAX 2550 VB/PC advance X-ray powder diffraction (<http://www.rigaku.com/en>, XRD, RIGAKU, Japan) with a $\text{Cu K}\alpha$ source. The 2θ angles probed were from 10° to 80° at a rate of 5° min^{-1} . The X-ray photoelectron spectra were obtained using an ESCALAB 250Xi X-ray photoelectron spectrometer (<https://www.thermofisher.com>, XPS, USA). The material element contents were determined by energy dispersive spectrometer (<http://www.edax.com>, EDS, Falcon, EDAX, USA). Nitrogen sorption/desorption isotherm was measured at 77 K with a Micromeritics Instrument Corporation TriStar II 3020 (<http://www.micromeritics.com>, USA). Before the sorption/desorption measurement, the samples were degassed in a vacuum at 300°C for 10 h. The Brunauer-Emmett-Teller (BET) method was used to calculate the specific surface area according to the adsorption data in a relative pressure from 0.06 to 0.30. The pore size distribution (PSD) was calculated based on the adsorption branch by using the Barrett-Joyner-Halenda (BJH) model. The quantification of Fe and Zr in the mesoporous carbon composite was performed by using inductively coupled plasma spectrometry with Radial ICP-OES equipment (<http://www.agilent.com/home>, ICP-OES, Agilent 725, USA).

Reagents and materials

Phenol, ethanol, acetylacetone, ammonium hydroxide, hydrochloric acid, sodium hydroxide, ammonium hydrogen carbonate and formalin solution (37 wt%) were analytical reagent grade and obtained from Sinopharm Chemical Reagent Co., Ltd. (<http://www.sinoreagent.com>, Shanghai, China). $\text{ZrO}(\text{NO}_3)_2 \cdot x\text{H}_2\text{O}$ was from Aladdin Chemical Reagent Co., Ltd. (<http://www.aladdin-e.com>, Shanghai, China). Poly(ethylene oxide)-block-poly(propylene oxide)-block-poly(ethylene oxide) triblock copolymer Pluronic F127 ($\text{PEO}_{106}\text{PPO}_{70}\text{PEO}_{106}$, $M_w = 12,600$), ferric acetylacetonate, β -casein (from bovine milk), bovine serum albumin (BSA), Trypsin (TPCK treated), dithiothreitol (DTT), iodoacetamide (IAA), urea, trifluoroacetic acid (TFA), Acetonitrile (ACN) and 2,5-dihydroxyl benzoic acid (DHB) were purchased from Sigma-Aldrich (<http://www.sigmaaldrich.com/china-mainland.html>, USA). These

reagents were at least of analytical-reagent grade and used as received without further treatment. Human serum from a healthy volunteer was provided by the Dalian Medical University and stored at $-80\text{ }^{\circ}\text{C}$ before analysis. Nonfat milk was obtained from a local supermarket. Pure water ($18.4\text{ M}\Omega\text{ cm}$) used in all experiments was purified by a Milli-Q system (<http://www.merckmillipore.com/CN/zh>, Millipore, Milford, MA, USA).

Preparation of the zirconia/magnetic mesoporous carbon composite

Soluble resol precursors were prepared by using phenol and formaldehyde via a base-catalyzed procedure according to the previously reported procedure [31]: 10 g phenol were heated to melt at $42\text{ }^{\circ}\text{C}$, then 2.13 g NaOH solution (20 wt%) was added slowly under stirring. After that, 17.7 g formalin solution (37 wt%) was added dropwise. The obtained mixture was heated at $75\text{ }^{\circ}\text{C}$ under stirring for 60 min. After the mixture was cooled down to room temperature, it was adjusted to pH 6 by hydrochloric acid solution. The mixture solution was dried by vacuum distillation at $50\text{ }^{\circ}\text{C}$ and centrifuged for removal of the produced NaCl. Then, the obtained resol precursor was redissolved in ethanol (20 wt%) for further use.

The metallic iron, ferric oxides and zirconia incorporated mesoporous carbon composites were synthesized through the chelate-assisted multi-components co-assembly strategy. The preparation was accomplished by gently evaporation of an ethanol solution containing Pluronic F127, resol, acetylacetone, ferric acetylacetonate and $\text{ZrO}(\text{NO}_3)_2 \cdot x\text{H}_2\text{O}$. In general, 0.5 g Pluronic F127 was dissolved in 7.0 g absolute ethanol. Then, 2.5 g resol precursor solution was added and the mixture was stirred for 10 min. 0.234 g $\text{ZrO}(\text{NO}_3)_2 \cdot x\text{H}_2\text{O}$ and 0.141 g ferric acetylacetonate were dissolved in 1.75 g ethanol. After that, 0.025 g acetylacetone solution was sequentially added dropwise into the above mixture solution. After stirring for 30 min, the mixture solution was cast onto a Petri dish, followed by evaporation of ethanol at room temperature for 12 h. Then the generated sticky film was heated at $100\text{ }^{\circ}\text{C}$ for 24 h. The resulting film was scrapped off and followed by calcinations in a tube furnace at $600\text{ }^{\circ}\text{C}$ for 3 h at a temperature ramp of $1\text{ }^{\circ}\text{C min}^{-1}$ under N_2 atmosphere. During the carbonization of resol precursor in the calcinations process, iron, ferric oxides and zirconia nanocrystallites were generated in situ.

Preparation of tryptic digests of standard proteins

1 mg β -casein or α -casein was dissolved in NH_4HCO_3 solution (1 mL , 50 mmol L^{-1}) and denatured by boiling for 5 min. Then, the denatured solution was incubated with trypsin (an enzyme/protein ratio of 1:40, w/w) for 16 h at $37\text{ }^{\circ}\text{C}$. The tryptic peptide mixtures were stored at

$-20\text{ }^{\circ}\text{C}$ for further use. The 2 mg BSA was denatured in urea (1 mL , 8 mol L^{-1}) and NH_4HCO_3 solution (1 mL , 50 mmol L^{-1}), followed by addition of DTT ($20\text{ }\mu\text{L}$, 1 mol L^{-1}) and incubating at $60\text{ }^{\circ}\text{C}$ for 1 h. Subsequently, 7.4 mg IAA was added and incubated at room temperature in the dark for 40 min. The mixture solution was diluted by ten-fold NH_4HCO_3 solution (50 mmol L^{-1}). Then, the protein was enzymolysis by trypsin with the same procedure of β -casein. The tryptic peptide solution was desalted by C18 SPE and dried by freeze until further use.

Preparation of human serum and tryptic digests of proteins extracted from non-fat milk

$20\text{ }\mu\text{L}$ of human serum was diluted by $120\text{ }\mu\text{L}$ water and denatured by boiling for 5 min. The denatured human serum was stored at $-20\text{ }^{\circ}\text{C}$ until further use. $30\text{ }\mu\text{L}$ of nonfat milk was added into NH_4HCO_3 solution (1 mL , 25 mmol L^{-1}) and centrifuged at 16000 rpm (17,930 g) for 15 min. The supernatant was collected and denatured by boiling for 5 min. The supernatant was digested with trypsin ($40\text{ }\mu\text{g}$) at $37\text{ }^{\circ}\text{C}$ for 16 h.

Enrichment of phosphopeptides

$200\text{ }\mu\text{g}$ of zirconia/magnetic mesoporous carbon composites were added into loading buffer (ACN- H_2O -TFA, 90:9:0.1, (v/v/v), $400\text{ }\mu\text{L}$) containing β -casein tryptic digest, α -casein tryptic digest, BSA tryptic digest, diluted human serum or digest of proteins extracted from nonfat milk, respectively. The mixture was gently incubated at room temperature for 30 min. After removing the supernatant by external magnet, the zirconia/magnetic mesoporous carbon composites were washed three times with loading buffer. The captured phosphopeptides were eluted by ammonium hydroxide ($20\text{ }\mu\text{L}$, 10 wt%) by powerful shaking for 15 min. The eluate was directly analyzed by MALDI-TOF MS.

Mass spectrometry analysis

All MALDI-TOF MS experiments were performed in the reflector positive mode by AB Sciex 4800 plus MALDI-TOF MS/MS mass spectrometer (<http://www.absciex.com.cn>, AB Sciex, USA) with a pulsed Nd/YAG laser at 355 nm. The DHB matrix was dissolved in ACN- H_2O - H_3PO_4 (70 : 29 : 1, (v/v/v), 25 mg). A $0.5\text{ }\mu\text{L}$ aliquot of the eluate and $0.5\text{ }\mu\text{L}$ of the DHB matrix were sequentially dropped onto the MALDI plate for MS analysis.

Results and discussion

Preparation and characterization of zirconia/magnetic mesoporous carbon composites

The preparation of zirconia/magnetic mesoporous carbon composites is illustrated in Scheme 1. Firstly, a soluble phenolic resin precursor (resol) was synthesized through a base-catalyzed procedure. Then, the zirconia/magnetic mesoporous carbon composites were synthesized through the chelate-assisted solvent evaporation induced co-assembly strategy. Finally, the decomposition film was pyrolyzed at 600 °C under N₂ atmosphere to remove template F127 and form the aligned mesopores. In the meanwhile, the resol framework was carbonized accompanied by in situ growth of metallic zirconia, iron and ferric oxides nanoparticles.

The structure and surface morphology of zirconia/magnetic mesoporous carbon composites were investigated with HR-TEM (Fig. S1, Electronic Supp. Material) and Ultrahigh Resolution Field Emission Scanning Electron Microscopy (Fig. S2, Electronic Supp. Material). The images of elements of Zr, Fe and O about zirconia/magnetic mesoporous carbon composites were observed through SEM. The quantification of Zr (7.9 wt%) and Fe (5.1 wt%) were determined by ICP-OES. The zirconia/magnetic mesoporous carbon composites were shown by XRD patterns. The valence states of element on the surface of the zirconia/magnetic mesoporous carbon composites were characterized by XPS spectra. The BET surface area and pore volume about zirconia/magnetic mesoporous composites were obtained by N₂ sorption/desorption curves. The magnetic properties of the zirconia/magnetic

mesoporous composites were studied by using a vibrating sample magnetometer at room temperature. Such results and discussion about characterization of the materials were supplied to the Electronic Supporting Material (ESM).

What's more, the zirconia/magnetic mesoporous carbon composites can be uniformly dispersed in water without precipitating after two days, showing excellent hydrophilicity, which benefits the enrichment of phosphopeptides in soluble biological sample. The OMC without metallic nanoparticles showed hydrophilicity too, which might be from oxidation of carbon material. But better hydrophilicity was observed after modified by zirconia and ferric oxide. Zirconia and ferric oxide are known for amphoteric property and have excellent hydrophilicity, which can react either as a Lewis acid or Lewis base depending on the pH of the reaction solution. Then the excellent hydrophilicity of magnetic mesoporous carbon nanocomposite may be from the joint effect of oxidation of mesoporous carbon and hydrophilic metallic zirconia, iron and ferric oxide.

Application in phosphopeptides enrichment

To demonstrate the practicability of the zirconia/magnetic mesoporous composites as the MOAC stationary phase for the enrichment of phosphopeptides, bovine β -casein (Fig. 1) and α -casein (Fig. 2) tryptic digests were used as standard phosphopeptides for enrichment. Protein tryptic digests were incubated with zirconia/magnetic mesoporous composites in loading buffer. The captured phosphopeptides were separated by external magnet and eluted after enrichment. Last, the droplet was deposited on the MALDI target for MALDI-

Scheme 1 Synthetic procedure of zirconia/magnetic mesoporous carbon composites

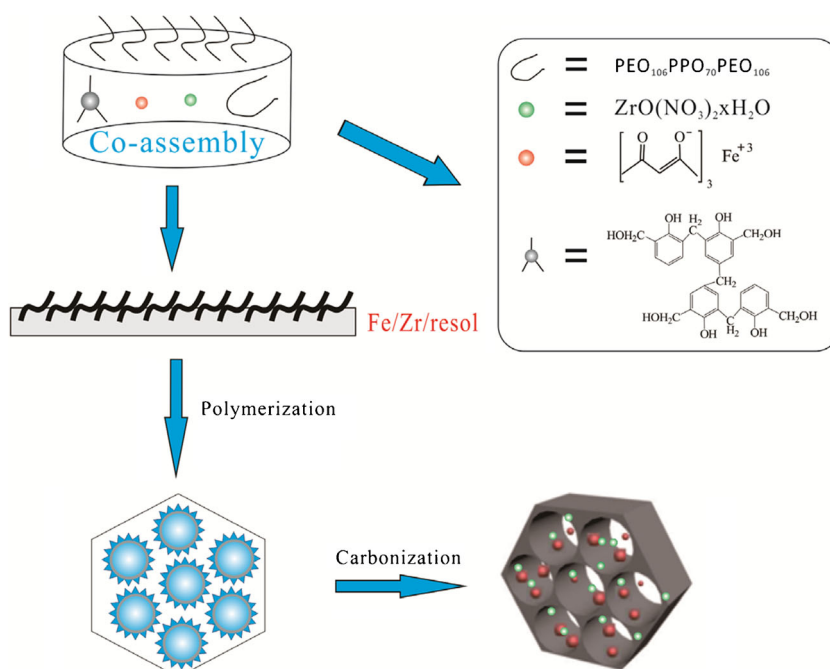
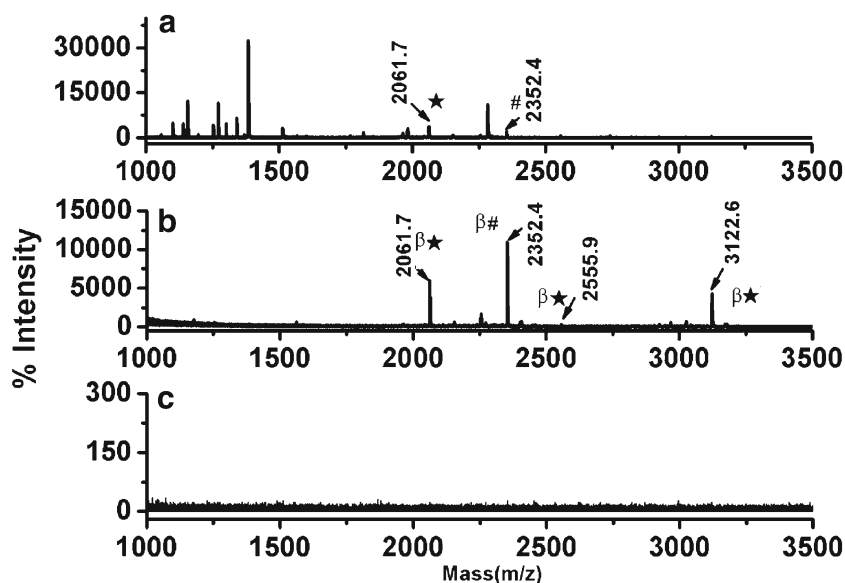


Fig. 1 MADIL-TOF mass spectra of the tryptic digests of β -casein. (a) Direct analysis (0.5 pmol) and (b) after enrichment by zirconia/magnetic mesoporous composites (1.0 pmol) and (c) ordered mesoporous carbon (0.5 pmol). * indicates phosphopeptides, # indicates dephosphopeptides, the β indicates phosphopeptide was from β -casein



TOF MS analysis. From parallel experiments ($n = 3$), the same three phosphopeptides and one dephosphopeptide could be detected every time for the enrichment of phosphopeptides from bovine β -casein after enriching by zirconia/magnetic mesoporous composites. And sixteen phosphopeptides were detected from bovine α -casein for three duplicate experiments too ($n = 3$), showing excellent reproducibility. The results indicated that irregular structure of mesoporous carbon had no effect on enrichment reproducibility.

As shown in Fig. 1a, owing to the low-concentration of phosphopeptides and signal suppression by abundant non-phosphopeptides, only two phosphopeptides with weak MS signal intensity and low signal-to noise (S/N) ratio were detected. However, after enrichment by zirconia/magnetic mesoporous composites (Fig. 1b), three phosphopeptides (m/z 2061.7, 2555.9 and 3122.6) could be clearly examined with

strong MS signal intensity and S/N ratio, along with dephosphopeptides (m/z 2352.4) which were likely to form during the ionization process by MALDI-TOF MS analysis. The detailed information of the captured phosphopeptides from β -casein digest was displayed in Table S1. By contrast, nearly no MS signal was enriched by ordered mesoporous carbon from β -casein tryptic digest (Fig. 1c). It well indicated that the metallic iron, ferric oxides and zirconia had the dominant effect during the enrichment process. Similarly, enrichment of α -casein digests by zirconia/magnetic mesoporous composites were illustrated in Fig. 2. Only several phosphopeptides were detected by direct analysis (Fig. 2a). After enriching by the zirconia/magnetic mesoporous composites, the strong MS intensity and S/N signals of phosphopeptides were highly enhanced with the removal of abundant non-phosphopeptides (Fig. 2b). Seventeen phosphopeptides and dephosphopeptides were identified including ten mono-phosphopeptides and six multi-phosphopeptides. Detailed information was displayed in Table S2.

To evaluate the high selectivity for the enrichment of phosphopeptides by the MOAC materials, mixtures of β -casein and BSA tryptic digests with different molar ratios were selected as testing sample. As shown in Fig. 3a, the mixture of β -casein and BSA (1:100) was directly examined, only showing non-phosphopeptides and hardly can see any phosphopeptides. Then, different molar ratios of β -casein and BSA tryptic digests (1:300 (b), 1:400 (c) and 1:500 (d)) were selected for enrichment by zirconia/magnetic mesoporous composites. As shown in Fig. 3d, when the molar ratio of β -casein and BSA was increased to 1:500, three expected phosphopeptides and the corresponding dephosphopeptides can still be identified with a clear background. Detailed information was shown in Table S3. Compared to our previous

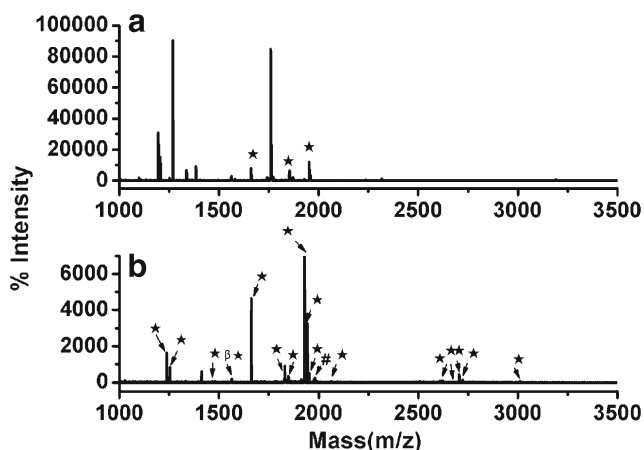
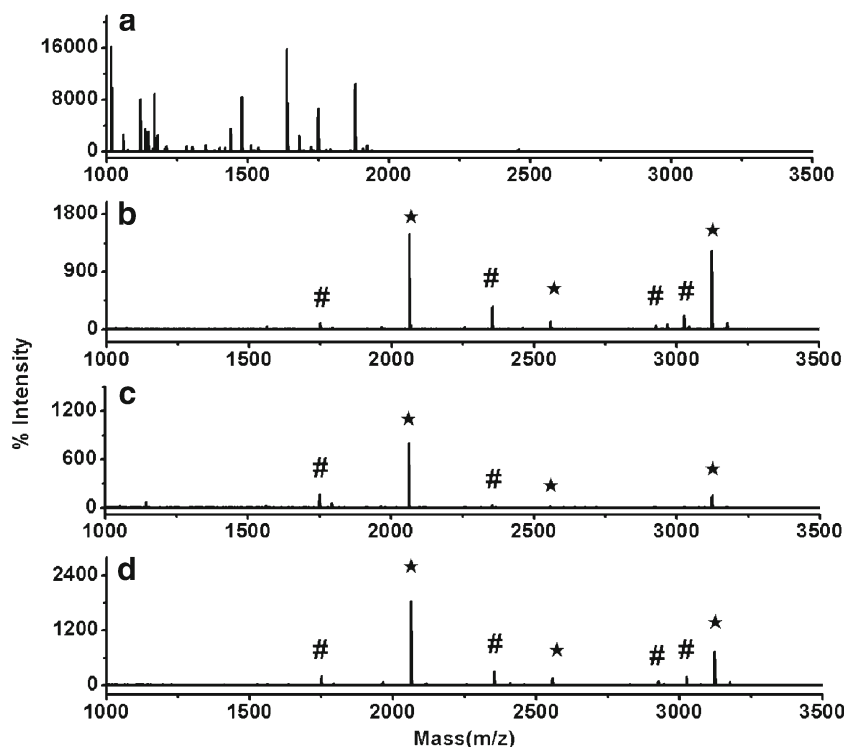


Fig. 2 MADIL-TOF mass spectra of the tryptic digests of α -casein. (a) Direct analysis (0.5 pmol) and (b) after zirconia/magnetic mesoporous composites (1.0 pmol) * indicates phosphopeptide, # indicates dephosphopeptide

Fig. 3 MALDI-TOF mass spectra of the tryptic digests mixture of β -casein and BSA before enrichment (a) 1:100 and after enrichment by zirconia/magnetic mesoporous composites at molar ratios of (b) 1 : 300, (c) 1 : 400, and (d) 1 : 500. * indicates phosphopeptide, # indicates dephosphopeptide

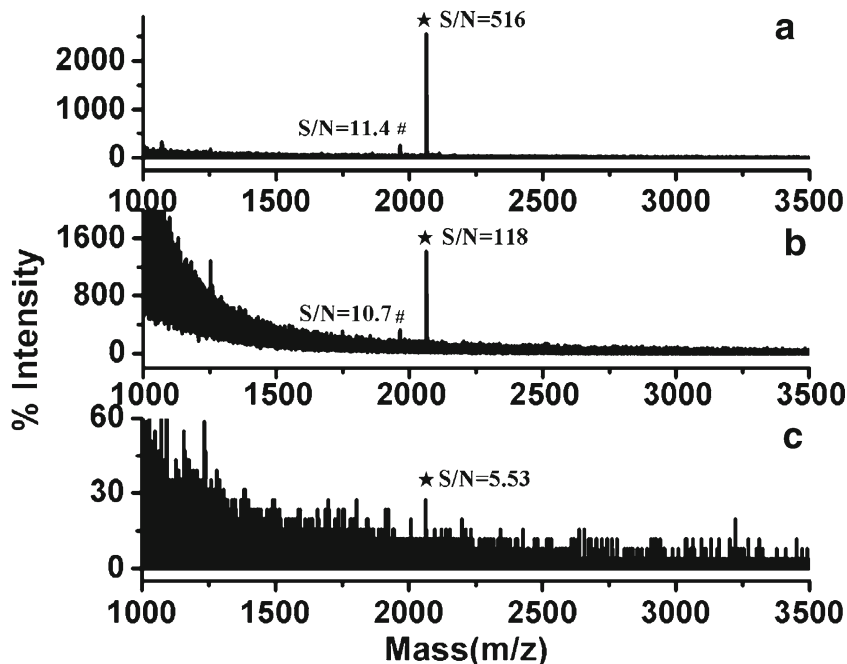


work, the selectivity of molar ratio of β -casein and BSA (1:500) was higher than the material of zirconia/OMC composites (1:300). It also contained less non-phosphopeptides. The above results indicated that material shown high selectivity in a complex peptide mixture, which mostly attributed to the loading of magnetic iron and ferric oxides.

The ability of enriching and detecting process is still a key task to evaluate the enrichment performance of the MOAC

materials due to the low abundance of phosphopeptides. Thus, concentration gradient of β -casein tryptic digest was given to evaluate the ability of zirconia/magnetic mesoporous composites. As shown in Fig. 4a, the peak with m/z of 2061.7 was clearly detected in 150 fmol of β -casein tryptic digest with the S/N ratio of 516. The dephosphopeptides at 1963 was also detected with S/N ratio of 11.4. A high S/N ratio of 118 can still be detected as the concentration decreased to the

Fig. 4 MALDI-TOF mass spectra of the tryptic digests of β -casein after enrichment by zirconia/magnetic mesoporous composites. (a) 150 fmol (0.5 μ L), (b) 15 fmol (0.5 μ L) and (c) 1.5 fmol (0.5 μ L). * indicates phosphopeptides



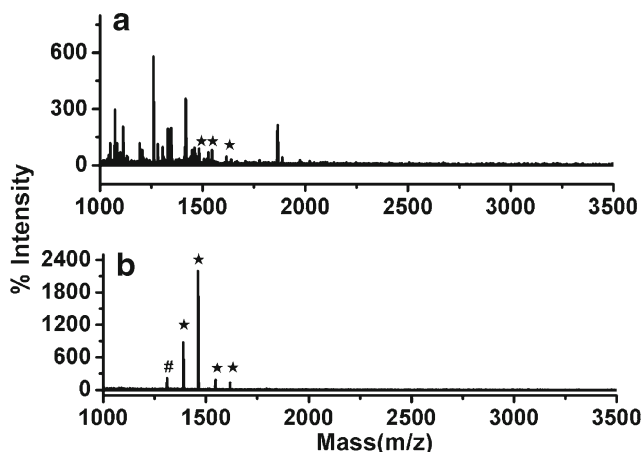


Fig. 5 MADIL-TOF mass spectra of diluted human serum. (a) Direct analysis and (b) after enrichment by zirconia/magnetic mesoporous carbon composites. *indicates phosphopeptide, # indicates dephosphopeptide

15 fmol (Fig. 4b). Even though the total amount of β -casein tryptic digest was as low as 1.5 fmol (Fig. 4c), the peak at 2061.7 can be clearly detected with the S/N ratio of 5.53. The determination of detection limit experience indicated that the zirconia/magnetic mesoporous composites had high detection sensitivity for phosphopeptides.

Application in enrichment of phosphopeptides from human serum and nonfat milk

Based on the excellent results from above-mentioned experiments, further investigation was introduced by application on real biological sample. Human serum and nonfat milk were then applied as model samples. As for the MS spectra of human serum showing in Fig. 5a, only three phosphopeptides with weak MS signal intensity appeared due to the

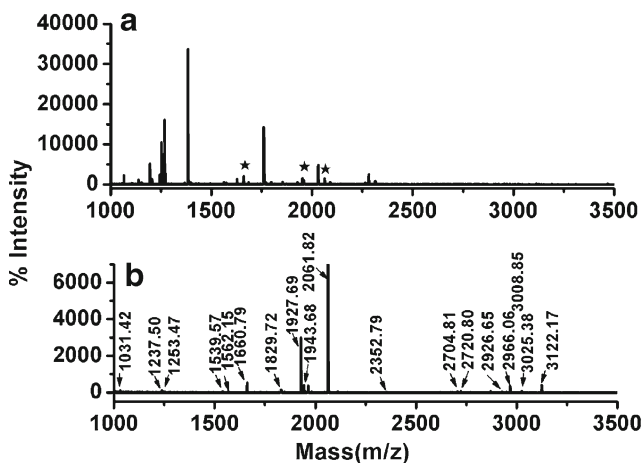


Fig. 6 MADIL-TOF mass spectra of tryptic digests of nonfat milk. (a) Direct analysis and (b) after enrichment by zirconia/magnetic mesoporous carbon composites. *indicates phosphopeptide

Table 1 The comparison of zirconia/magnetic mesoporous carbon composite to other nanomaterials reported previously for capturing low-abundance phosphopeptides

Material	Method	Surface area ($\text{m}^2 \text{g}^{-1}$)	Content of metal element	LOD	Specificity (ratios of β -casein and BSA)	Identified phosphopeptides (nonfat milk)	Separation mode	Ref
$\text{Fe}_3\text{O}_4 @ \text{SiO}_2 @ (\text{HA}/\text{CS})_{10} \cdot \text{Ti}^{4+}$	IMAC	-	Ti: 44.38 $\mu\text{g mg}^{-1}$	0.5 fmol	1:2000	11	Magnetic separation	[7]
Urea-modified MIL-101 (Cr)	Amine-based affinity	1253	-	10^{-10} M	1:200	9	centrifugal separation	[17]
BaTiO_3	MOAC	-	-	-	-	21	centrifugal separation	[25]
ZrO_2 -MSN	MOAC	357	-	2.5 fmol	1:100	16	centrifugal separation	[29]
ZrO_2 -NP	MOAC	-	-	-	-	9	centrifugal separation	[29]
Zirconia/OMC	MOAC	387	Zr: 3.5 wt%	1.5 fmol	1:300	15	centrifugal separation	[30]
α - ZrO_2 -NP	MOAC	-	-	2 fmol	-	13	centrifugal separation	[35]
Ti^{4+} -G@PD	IMAC	-	6.76 wt%	1 fmol	1:1000	-	centrifugal separation	[36]
$\text{Fe}_3\text{O}_4 @ \text{fTiO}_2$	MOAC	50.45	-	5×10^{-10} M	1:1000	-	Magnetic separation	[37]
Ti^{4+} -ATP-MNPs	IMAC	-	-	3 amol	1:5000	-	Magnetic separation	[38]
Zirconia/magnetic mesoporous carbon	MOAC	442	Zr: 7.9 wt%, Fe: 5.1 wt%	1.5 fmol	1:500	18	Magnetic separation	This work

interference of abundant non-phosphopeptides and high salt content. However, after enrichment by zirconia/magnetic mesoporous composites (Fig. 5b), many non-phosphopeptides peaks disappeared, and four peaks of phosphopeptides and one peak of dephosphopeptides were examined with high intensity of MS signals. The detailed information of the captured phosphopeptides from diluted human serum is displayed in Table S4.

Similarly, the direct analysis results of the digested nonfat milk by MALDI-TOF MS are shown in Fig. 6a, only several weak MS signal of phosphopeptides can be seen. However, eighteen peaks MS of phosphopeptides were identified after enrichment by zirconia/magnetic mesoporous composites including eight mono-phosphopeptides and ten multi-phosphopeptides (Fig. 6b) [32–34]. The detailed information of phosphopeptides from the tryptic digest of proteins extracted from nonfat milk is given in Table S5. More phosphopeptides (18 vs 15) were enriched and detected by the zirconia/magnetic mesoporous carbon composites compare to our previous work by removing high abundant of non-phosphopeptides. It may be relevant to the joint effect of iron and ferric oxides and the lossless of magnetic separation during enrichment. The results indicated that zirconia/magnetic mesoporous composites can be selected an appropriate candidate for effectively and selectively capturing of phosphopeptides from a naturally complex biological sample.

To compare with other materials reported previously, multiple characters of the prepared material and others including the surface area, content of metal, LODs, specificity, number of identified phosphopeptides (nonfat milk) and separation mode were compared in Table 1. The zirconia/magnetic mesoporous carbon composite and related method had advantages in surface area, content of metal, LODs, numbers of identified phosphopeptides. The process of preparation and operation were also relatively simple and costless. However, the prepared material has limitation too. It could not be used to distinguish between multiphosphopeptides and monophosphopeptides as guanidyl-functionalized magnetic polymer microsphere [32].

Conclusions

In this work, the metallic iron, ferric oxides and zirconia incorporated mesoporous carbon were prepared. The zirconia/magnetic mesoporous carbon composites own large mesopores (4.8 nm), high surface area ($442 \text{ m}^2 \text{ g}^{-1}$), large pore volume ($0.37 \text{ cm}^3 \text{ g}^{-1}$), high loading content of metallic zirconia (7.9 wt%) and iron element (5.1 wt%) and high hydrophilicity. The metallic nanoparticles iron and ferric oxides which were introduced to the surface of mesoporous carbon, acted as both the source of the magnetic force for magnetic separation and the metal oxide affinity chromatography

material for the enrichment low-abundance phosphopeptides. The material improved the selectivity (1:500) and sensitivity (1.5 fmol) for enrichment phosphopeptides. For the selective enrichment of phosphopeptide from human serum and nonfat milk, the zirconia/magnetic mesoporous carbon composites displays excellent practicability in identifying low abundance phosphopeptide from complex biological sample.

Acknowledgements This work was financially supported by the State Key Program of National Natural Science of China (21235005), the National Key Scientific Instrument and Equipment Development Project (2012YQ120044), the National Natural Science Foundation of China (21475044), the model Project of the Research and Application of the Common Key Technology about Chemical Reagent of Basis Scientific Research (2015BAK44B00) and foundation of Shanghai Research Institute of Criminal Science and Technology.

Compliance with ethical standards The author(s) declare that they have no competing interests.

References

- Pawson T, Scott JD (2005) Protein phosphorylation in signaling—50 years and counting. *Trends Biochem Sci* 6:286
- Hunter T (2005) Signaling—2000 and Beyond. *Cell* 100:113
- Liu CM, Li YM, Semenov M, Han C, Baeg GH, Tan Y, Zhang ZH, Lin XH, He X (2002) Control of β -catenin phosphorylation/degradation by a dual-kinase mechanism. *Cell* 108:837
- Liu F, Iqbal K, Iqbal IG, Hart GW, Gong CX (2004) O-GlcNAcylation regulates phosphorylation of tau: a mechanism involved in Alzheimer's disease. *Proc Natl Acad Sci* 101:10804
- Danielsson A, Ost A, Nystrom FH, Stalfors P (2005) Attenuation of insulin-stimulated insulin receptor substrate-1 serine 307 phosphorylation in insulin resistance of type 2 diabetes. *J Biol Chem* 280:34389
- Chen YJ, Xiong ZC, Peng L, Gang YY, Zhao YM, Shen J, Qian JH, Zhang LY, Zhang WB (2015) Facile preparation of Core-Shell magnetic metal-organic framework nanoparticles for the selective capture of phosphopeptides. *ACS Appl Mater Interfaces* 7:16338
- Xiong ZC, Zhang LY, Fang CL, Zhang QQ, Ji YS, Zhang Z, Zhang WB, Zou HF (2014) Ti^{4+} -immobilized multilayer polysaccharide coated magnetic nanoparticles for highly selective enrichment of phosphopeptides. *J Mater Chem B* 2:44730
- Liu W, Zheng JN, Li SH, Wang RR, Lin Z, Yang HH (2015) Aluminium glycinate functionalized silica nanoparticles for highly specific separation of phosphoproteins. *J Mater Chem B* 3:6528
- Xu L, Zhu W, Sun R, Ding Y (2015) A Ti^{4+} -immobilized phosphate polymer-patterned silicon substrate for on-plate selective enrichment and self-desalting of phosphopeptides. *Analyst* 140:3216
- Zheng LY, Dong HP, Hu LJ (2013) Zirconium-cation-immobilized Core/Shell (Fe_3O_4 @polymer) microspheres as an IMAC material for the selective enrichment of phosphopeptides. *Ind Eng Chem Res* 52:7729
- Chen Y, Li DJ, Bie ZJ, He XP, Liu Z (2016) Coupling of phosphate-imprinted mesoporous silica nanoparticles-based selective enrichment with matrix-assisted laser desorption ionization-time-of-flight mass spectrometry for highly efficient analysis of protein phosphorylation. *Anal Chem* 88:1447
- Qin YP, Li DY, He XW, Li WY, Zhang YK (2016) Preparation of high-efficiency cytochrome c-imprinted polymer on the surface of

- magnetic carbon nanotubes by epitope approach via metal chelation and six-membered ring. *ACS Appl Mater Interfaces* 8:10155
13. Tseng HC, Ovaa H, Wei NJC, Ploegh H, Tsai LH (2015) Phosphoproteomic analysis with a solid-phase capture-release-tag approach. *Chem Biol* 12:769
 14. Hennrich ML, Toorn HWP, Groenewold V, Heck AJR, Mohammed S (2012) Ultra acidic strong cation exchange enabling the efficient enrichment of basic phosphopeptides. *Anal Chem* 84:1804
 15. Zarei M, Sprenger A, Gretzmeier C, Dengjel J (2012) Polydopamine-coated magnetic nanoparticles for enrichment and direct detection of small molecule pollutants coupled with MALDI-TOF-MS. *J Proteome Res* 11:4269
 16. Alpert AJ, Hudecz O, Mechtler K (2015) Anion-exchange chromatography of phosphopeptides: weak anion exchange versus strong anion exchange and anion-exchange chromatography versus electrostatic Repulsion – Hydrophilic interaction chromatography. *Anal Chem* 87:4704
 17. Yang XQ, Xia Y (2016) Urea-modified metal-organic framework of type MIL-101(Cr) for the preconcentration of phosphorylated peptides. *Microchim Acta* 183:2235
 18. Liu HL, Yang TY, Dai JY, Zhu JY, Li XR, Wen R, Yang XH (2015) Hydrophilic modification of titania nanomaterials as a biofunctional adsorbent for selective enrichment of phosphopeptides. *Analyst* 140:6652
 19. Wang ZG, Lv N, Bi WZ, Zhang JL, Ni JZ (2015) Development of the affinity materials for phosphorylated proteins/peptides enrichment in Phosphoproteomics analysis. *ACS Appl Mater Interfaces* 7: 8377
 20. Hu Y, Shan CX, Wang J, Zhu JM, Gu CQ, Ni WT, Zhu D, Zhang AH (2015) Fabrication of functionalized SiO₂/TiO₂ nanocomposites via amidation for the fast and selective enrichment of phosphopeptides. *New J Chem* 39:6540
 21. Ma WF, Zhang C, Zhang YT, Yu M, Guo J, Zhang Y, Lu HJ, Wang CC (2014) Magnetic MSP@ZrO₂ microspheres with yolk–Shell structure: designed synthesis and application in highly selective enrichment of phosphopeptides. *Langmuir* 30:6602
 22. Zhang YT, Li LL, Ma WF, Zhang Y, Yu M, Guo J, Lu HJ, Wang CC (2013) Two-in-one strategy for effective enrichment of phosphopeptides using magnetic mesoporous γ -Fe₂O₃ Nanocrystal clusters. *ACS Appl Mater Interfaces* 5:614
 23. Çelikbıçak Ö, Atakay M, Güler Ü, Salih B (2013) A novel tantalum-based sol-gel packed microextraction syringe for highly specific enrichment of phosphopeptides in MALDI-MS applications. *Analyst* 138:4403
 24. Huang X, Wang JP, Wang JY, Liu CC, Wang S (2015) Preparation of graphene–hafnium oxide composite for selective enrichment and analysis of phosphopeptides. *RSC Adv* 5:89644
 25. Kailasa SK, Wu HF (2012) Rapid enrichment of phosphopeptides by BaTiO₃ nanoparticles after microwave-assisted tryptic digest of phosphoproteins, and their identification by MALDI-MS. *Microchim Acta* 179:83
 26. Long XY, Song Q, Lian HZ (2015) Development of magnetic LuPO₄ microspheres for highly selective enrichment and identification of phosphopeptides for MALDI-TOF MS analysis. *J Mater Chem B* 3:9330
 27. Pang H, Lu Q, Gao F (2011) Graphene oxide induced growth of one-dimensional fusiform zirconia nanostructures for highly selective capture of phosphopeptides. *Chem Commun* 47:11772
 28. Wan H, Li JA, Yu WG, Liu ZY, Zhang QQ, Zhang WB, Zou HF (2014) Fabrication of a novel magnetic yolk–shell Fe₃O₄@mTiO₂@mSiO₂ nanocomposite for selective enrichment of endogenous phosphopeptides from a complex sample. *RSC Adv* 4:45804
 29. Zhang XL, Wang F, Xia Y (2013) Trypsin functionalization and zirconia coating of mesoporous silicananotubes for matrix-assisted laser desorption/ionization massspectrometry analysis of phosphoprotein. *J Chromatogr A* 1306:20
 30. Zhang L, Xiong ZC, Chen YJ, Peng L, Yu BH, Gao XD, Zhang RS, Zhang LY, Zhang WB (2016) Soft-template synthesis of hydrophilic metallic zirconia nanoparticle-incorporated ordered mesoporous carbon composite and its application in phosphopeptide enrichment. *RSC Adv* 6:30014
 31. Sun ZK, Sun B, Qiao MH, Wei J, Yue Q, Wang C, Deng YH, Kaliaguine S, Zhao DY (2012) A general chelate-assisted Co-assembly to metallic nanoparticles-incorporated ordered mesoporous carbon catalysts for Fischer–Tropsch synthesis. *J Am Chem Soc* 134:17635
 32. Xiong ZC, Chen YJ, Zhang LY, Ren J, Zhang QQ, Ye ML, Zhang WB, Zou HF (2014) Facile synthesis of guanidyl-functionalized magnetic polymer microspheres for tunable and specific capture of global phosphopeptides or only multiphosphopeptides. *ACS Appl Mater Interfaces* 24:22743
 33. Lu ZD, Duan JC, He L, Hu YX, Yin YD (2010) Mesoporous TiO₂ Nanocrystal clusters for selective enrichment of phosphopeptides. *Anal Chem* 82:7249
 34. Atakay M, Celikbıçak O, Salih B (2012) Amine-functionalized Sol–gel-based lab-in-a-pipet-tip approach for the fast enrichment and specific purification of phosphopeptides in MALDI-MS applications. *Anal Chem* 84:2713
 35. Kailasa SK, Wu HF (2010) Multifunctional ZrO₂ nanoparticles and ZrO₂-SiO₂ nanorods for improved MALDI-MS analysis of cyclodextrins, peptides, and phosphoproteins. *Anal Bioanal Chem* 396: 1115
 36. Yan YH, Zheng ZF, Deng CH, Li Y, Zhang XM, Yang PY (2013) Hydrophilic Polydopamine-coated graphene for metal ion immobilization as a novel immobilized metal ion affinity chromatography platform for Phosphoproteome analysis. *Anal Chem* 85:8483
 37. Cheng G, Wang ZG, Liu YL, Zhang JL, Sun DH, Ni JZ (2013) Magnetic affinity microspheres with Meso–/Macroporous shells for selective enrichment and fast separation of phosphorylated biomolecules. *ACS Appl Mater Interfaces* 5:3182
 38. Zhang LY, Zhao Q, Liang Z, Yang KQ, Sun LL, Zhang LH, Zhang YK (2012) Synthesis of adenosine functionalized metal immobilized magnetic nanoparticles for highly selective and sensitive enrichment of phosphopeptides. *Chem Commun* 48:6274